Optimum Design Parameters for Ultra-Low-Power RF Transceivers in Wireless Sensor Networks

MHD Zaher Mahfouz, Arjan Meijerink, and Mark J. Bentum
University of Twente, Telecommunication Engineering Group
P.O. Box 217, 7500 AE, Enschede, The Netherlands
Email: {z.mahfouz, a.meijerink, m.j.bentum}@utwente.nl

***Abstract*—In wireless sensor networks, the need for ultra-low power consuming nodes is one of the main motivations for research in such field. Because radio sections in sensor nodes contribute to a large extent to the overall power consumption, the focus of this study is on the RF transceiver. The aim is to reduce the average power consumption which depends significantly on the circuit architecture design, operating data rate, and duty cycle. In a symmetric communicating system, due to the tradeoff between transmitting power and receiver sensitivity on one hand, as well as between phase noise tolerance and power dissipation in local oscillators on the other hand, the design and operating parameters of the transceiver need to be determined from the perspective of the average power consumption. Therefore, in our study, as an initial step in system design, the optimum for instantaneous data rate, noise figure, and oscillator power budget are analytically determined. The analysis is carried out, taking into consideration an existing in-channel wideband interference, on two transceiver architectures: RF envelope detection and conventional heterodyne. The transceiver in both architectures employs on-off-keying modulation and duty cycling. The optimums are then calculated numerically based on design constants obtained from a frequently-cited RF envelope transceiver, indicating that an energy efficiency improvement of up to 5 dB can still be achieved.**

Keywords—energy efficiency; envelope detection; heterodyne; OOK; optimization; phase noise; RF section; tradeoff; transceiver; ultra-low power; wireless sensor network

I. INTRODUCTION

The key considerations that drive the competition in the market of wireless sensor networks (WSNs) are cost, size and power consumption. In research, the latter is considered to be the most important factor as it essentially determines the size of the battery that must be used to power the sensor node, and, accordingly, the overall size of the node itself [1]. Additionally, the power consumption drastically influences the lifetime of the sensor nodes, whose batteries cannot be recharged or even replaced once they are depleted, as this would not be cost-efficient for large networks. Moreover, due to the size constraint in some specific WSN applications, sensor nodes cannot use batteries at all, but solely depend on energy scavenging from the surrounding environment (e.g. vibrations, heat and light) [2]. To make such applications feasible and to extend the node lifetime as much as possible, ultra-low-power (ULP) design is highly demanded. Otherwise, many WSN applications could still not be widely adopted.

Common radio standards, such as Wi-Fi, Bluetooth and ZigBee, have spawn much research, and they are already widely established and deployed in a variety of commercial applications. However, they are not preferred for WSN radios because they tend to produce power-hungry nodes [3], so the battery lifetime might then be up to only several months in a best-case scenario. Even though ZigBee technology was aimed at low-power radio devices, it still consumes an average power in the order of milliwatts, and, therefore, it is not suitable for sensor nodes that depend on energy scavenging. Since there is no available standard for ULP radios, it has become a hot research topic in recent years. Therefore, many systems and schemes have been proposed. However, such systems are usually designed and then tested under laboratory conditions where there is no interference. In practice, there might be interference from adjacent channels as well as from other systems sharing the same frequency band. In order to overcome such interference, an additional power must be consumed by the transmitting and/or receiving nodes. Consequently, the design and operating parameters might need to be modified to keep the node power consumption as low as possible.

To tackle the challenge of power consumption, there has been much research and many innovative ideas in ULP design spanning from the network layer (e.g. energy-efficient routing protocols [4]), through the media-access control layer [5], and down to the physical (PHY) layer. Because radio sections in sensor nodes contribute to the overall energy dissipation to a large extent [6, 7], research has focused on radio design to achieve low-power transceivers by following different approaches. One of them is to investigate the power consumption of different RF blocks and try to come up with energy consumption models (as in [8-10]) subject to a number of conditions. Using these models, existing design tradeoffs can be combined together to find the optimum values for some design and operating parameters from the energy efficiency perspective. For example, in [8], a formula for the optimum power consumption of the low-noise amplifier (LNA) was introduced for a given indoor propagation model, transceiver power budget, and fixed bandwidth. For a given link budget, there is a tradeoff between transmitter (TX) instantaneous radiated power and receiver (RX) sensitivity. Another tradeoff exists between instantaneous data rate and duty cycle for a

978-1-5090-1328-9/16/$31.00 ©2016 IEEE

desired average data rate. In [9], both previously-mentioned tradeoffs were combined in one analysis to minimize the total average power consumption in a duty-cycled transceiver. Li et al. in [10] studied the conventional RF architectures for four different modulation techniques (on-off keying, phase-shift keying, quadrature amplitude modulation, and frequency-shift keying). For each modulation, they presented a model for the consumed energy per bit, and optimized for different bandwidth (narrow, medium, or wide) and data rate (low, middle, or high) requirements. For every requirement and intended transmission range, they found an optimal modulation scheme with which the energy efficiency was maximized.

The aim of our study is to minimize the total average power consumption in the transceiver circuit as a whole, by determining three optimum design parameters, namely instantaneous data rate, receiver noise figure, and local oscillator (LO) power budget. Therefore, the two previously-mentioned tradeoffs, that were considered in [9], are applied in one analysis for an RF envelope detector-based transceiver. In another analysis, we consider an additional tradeoff which exists between the phase noise tolerance and LO power budget [11] for a conventional heterodyne-based transceiver. Because many WSN applications are deployed in the crowded 2.4-GHz ISM band, we also consider an in-channel wideband interference in both analyses. We then apply the analysis of the two architectures on a numerical example to gain more insight on the theoretical outcome. Our main contribution is combining the three tradeoffs (instantaneous radiated power vs. receiver sensitivity, duty cycle vs. instantaneous data rate, and LO power budget vs. phase noise) in one analysis, taking into account an in-channel wideband interference.

The remaining of the paper is organized as follows. Section II provides the theoretical analysis for the optimization of the total average power consumption in the RF envelope detection and the conventional heterodyne-based transceivers. A numerical example and a discussion are given in Section III for the analysis of both architectures. A conclusion is provided in the end with a motivation for further research.

II. Theoretical Analysis

In radio design, there are multiple tradeoffs that need to be considered simultaneously in order to cut down on the total average power consumption. 1) For a given link budget L_{B}, improving the sensitivity P_{sens} of the RX reduces the required instantaneous radiated power P_{rad} at the TX, and, as a result, decreases the power consumption in the TX. However, achieving better sensitivity needs more power to be consumed in the RX in order to improve its noise figure. Therefore, the tradeoff between P_{rad} and P_{sens} needs to be considered. 2) To decrease the average power consumption in both the TX and the RX, a duty-cycling technique is usually employed. For a given WSN application, in which the packet length N_{b} and the average packet rate R_{p} are specified (i.e. the average data rate is fixed), decreasing the duty cycle reduces the average power consumption. Because the instantaneous data rate R_{b} is inversely proportional to the duty cycle, decreasing the latter means higher operating R_{b} and thereby requires greater P_{rad} as a consequence. However, P_{rad} is upper-limited by practical

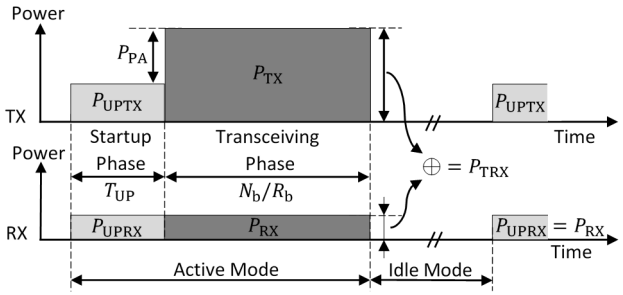

Fig. 1. The power consumption in the TRX. (P_{UPTX} and P_{UPRX} are the power consumption during the startup phase in the TX and RX, respectively. P_{TX} and P_{RX} are the power consumption during the transceiving phase in the TX and RX, respectively.)

factors such as emission regulations and battery capabilities [12]. Consequently, the upper limit on P_{rad} yields an upper limit on R_{b}. Aside from this practical upper limit, the required time T_{UP} for the startup phase results in an associated energy consumption E_{UP} which increases with higher operating R_{b}, due to power dissipation in baseband circuits. As a result, at the beginning of increasing R_{b} (by decreasing the duty cycle), the total average power consumption begins to reduce, but later, at a specific point, it starts to increase [13]. Therefore, R_{b} cannot be increased arbitrarily and it has to be traded off against duty cycle. 3) The phase noise of LOs in RXs causes adjacent-channel interference and degrades the bit error rate (BER) performance as well. To compensate for the degradation and to mitigate the interference, either P_{rad} at the TX is increased or the phase noise performance of the LO in the RX is improved. In fact, improving the phase noise performance alleviates the required P_{rad}, but necessitates more power to be dissipated in LOs which are considered among the power-hungry blocks in RF front ends.

In our study, the optimization for the total average power consumption is carried out on the node level of a symmetric communicating system (i.e. peer to peer), in which our analysis only takes the PHY layer of the RF transceiver into consideration. The aim is to determine the minimum consumed energy per transceived bit $E_{\mathrm{bit,min}}$, along with the corresponding optimum operating and design parameters, for the case of duty-cycled burst communications in which a packet is to be delivered from a transmitting node to a receiving node. The consumed energy per transceived bit E_{bit} is defined to be the effective energy that is dissipated in the *transceiver circuits of both the TX and the RX* (TRX), for every channel bit to be delivered in between. E_{bit} is thereby defined as $E_{\mathrm{bit}} = E_{\mathrm{pkt}}/N_{\mathrm{b}}$, where E_{pkt} is the total consumed energy in the TRX (during the startup and transceiving phases) per transceived packet. In fact, for a given required average bit rate, minimizing E_{bit} gives the same outcome if we do it from the perspective of the total average power consumption. Fig. 1 shows the power consumption in the TRX over time. Due to duty cycling, the idle mode has a negligible power consumption as the node is put into sleep. On the other hand, the active mode consists of two power-consuming phases, namely the startup phase and the transceiving phase. Only a single packet is delivered in one way per active mode. As opposed to [9], we assume that the power consumption in the TRX during the transceiving phase is equal

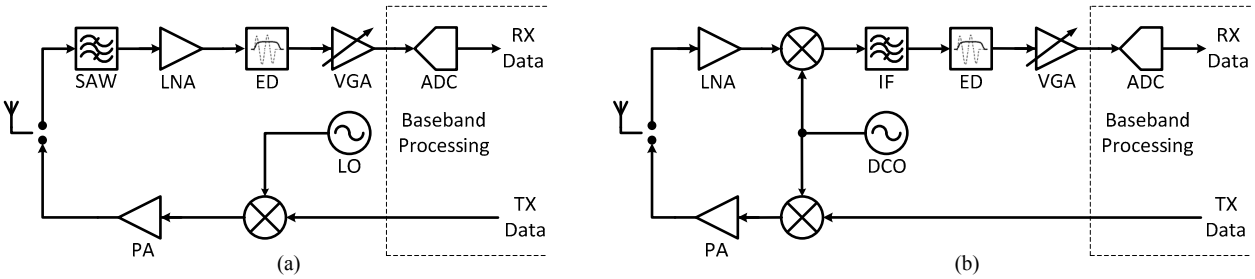

Fig. 2. The block diagram of the (a) RF envelope detector and (b) heterodyne based transceivers.

to that during the startup phase except for the portion P_{PA} which corresponds to the power consumption of the power amplifier (PA) in the TX. Therefore, E_{bit} is expressed as

$$E_{\mathrm{bit}} = \frac{1}{N_{\mathrm{b}}}\left[P_{\mathrm{TRX}}\left(T_{\mathrm{UP}} + \frac{N_{\mathrm{b}}}{R_{\mathrm{b}}}\right) - P_{\mathrm{PA}}T_{\mathrm{UP}}\right], \quad (1)$$

where P_{TRX} is the power consumption in the TRX during the transceiving phase.

The block diagram of the transceiver, which is duty cycled, is shown in Fig. 2(a) and 2(b), for the RF envelope detection and the heterodyne architectures, respectively. The TX section is simplified in both architectures. The adopted modulation scheme in both is on-off-keying (OOK), whose BER is more immune—when envelope detection is implemented—to phase noise compared to other modulation schemes such as phase shift keying. The power consumptions in baseband circuits [14, 15], LNA [8], and PA are given by

$$P_{\mathrm{BB}} = k_{\mathrm{ADC}}R_{\mathrm{b}} + k_{\mathrm{DC}}R_{\mathrm{b}} = k_{\mathrm{BB}}R_{\mathrm{b}}, \quad (2)$$

$$P_{\mathrm{LNA}} = \frac{K_{\mathrm{LNA}}}{F_{\mathrm{LNA}}-1}, \quad (3)$$

$$P_{\mathrm{PA}} = \frac{1}{\rho}P_{\mathrm{rad}}, \quad (4)$$

where k_{ADC}, k_{DC} and k_{BB} (expressed in watt/bps) are the consumed energy per transceived bit in the ADC, digital circuits, and both, respectively, F_{LNA} is the noise factor of the LNA, k_{LNA} (expressed in watt) is the required P_{LNA} to achieve $F_{\mathrm{LNA}} = 2$, and ρ is the PA efficiency. $k_{\mathrm{BB}}, k_{\mathrm{LNA}}$, and ρ are design constants. Equation (2) represents the dynamic power consumption in the digital circuits and the ADC, whereas the static power consumption (due to leakage current) is neglected. The clock frequency of baseband circuits linearly scales with the operating data rate, depending on the resolution and the number of instructions that are required to process a single transceived bit. Equation (3) is valid for LNAs that are implemented in MOSFET biased in saturation [8, 16], and whose design parameters (e.g. gain and linearity) are assumed to be fixed.

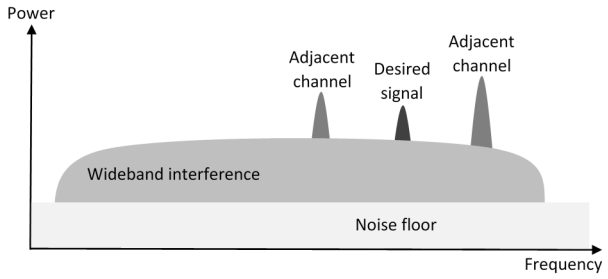

Fig. 3. Power spectrum of the operating frequency band.

For a given L_{B}, the minimum required received signal strength P_{RSS} is related to P_{rad} [17] as in

$$P_{\mathrm{rad}} = \frac{PL}{G_{\mathrm{TX}}G_{\mathrm{RX}}}P_{\mathrm{RSS}} = L_{\mathrm{B}}P_{\mathrm{RSS}}, \quad (5)$$

where G_{TX} and G_{RX} are the antenna gains for the TX and the RX, respectively, and PL is the maximum allowable path loss. The receiver sensitivity is given by

$$P_{\mathrm{sens}} = k_{\mathrm{B}}T_0F_{\mathrm{eq}}B_{\mathrm{eq}}SNR_{\mathrm{min}}, \quad (6)$$

where k_{B} is Boltzmann's constant, T_0 is the room temperature, F_{eq} is the total standard noise factor of the RX, B_{eq} is the equivalent noise bandwidth of the RX, and SNR_{min} is the minimum signal-to-noise ratio that is required to achieve a specific BER value. For the case of the heterodyne architecture shown in Fig. 2(b), because F_{LNA} usually dominates F_{eq} in Friis' formula [17], the latter can be safely replaced by the former in (6). B_{eq} is determined by the bandwidth of the intermediate filter B_{IF}, which itself is associated together with R_{b} through the spectral efficiency η (i.e. $B_{\mathrm{eq}} = B_{\mathrm{IF}} = R_{\mathrm{b}}/\eta$). On the other hand, for the case of the RF envelope detection architecture shown in Fig. 2(a), F_{eq} is not straightforward as it cannot be simply obtained from Friis' formula. This is due to the fact that the bandwidth of the SAW filter is much smaller than that of the LNA. Nevertheless, assuming that the SAW filter (a passive device) is at room temperature, we can write $F_{\mathrm{eq}}B_{\mathrm{eq}} = L_{\mathrm{SAW}}[B_{\mathrm{SAW}} + (F_{\mathrm{LNA}} - 1)B_{\mathrm{LNA}}]$ according to the analysis of the equivalent input noise temperature, where L_{SAW} and B_{SAW} are the insertion loss and the bandwidth of the SAW filter, respectively, and B_{LNA} is the bandwidth of the LNA. An in-channel wideband interference is assumed to co-exist alongside with the desired signal as depicted in Fig. 3. In our analysis, the wideband interference is modelled as a zero-mean white Gaussian process with a single-sided power spectral density (PSD) of I_0.

The study is split into two analyses. In the first one, we consider the architecture of the RF envelope detector-based transceiver, whereas in the second analysis, we consider the heterodyne architecture. In both analyses, we make the following assumptions. 1) The transmitting and receiving nodes are perfectly synchronized. 2) The necessary synchronization bits are already included in the packet format and their number is independent of R_{b}. 3) The power consumption during idle (sleep) mode is neglected compared to that during the active (wakeup) mode. 4) Although T_{UP} is mainly dominated by the

LO, here we assume that it is constant and not dependent on the amount of power P_{osc} dissipated in the LO. 5) The RX' spurious-free dynamic range (SFDR) is large enough to avoid intermodulation distortion. 6) The WSN application is given in which N_{b}, R_{p}, and L_{B} are already specified. In other words, the required average bit rate and the transmission range are fixed.

A. RF Envelope Detector-Based Transceiver

In this analysis, we consider the architecture of the RF envelope detection [13] for the sake of minimizing the total average power consumption of the TRX. Consequently, two tradeoffs apply to this analysis. The first one is between P_{rad} at the TX and P_{sens} of the RX. The second tradeoff is between R_{b} and duty cycle.

The power consumption in the TRX during the transceiving phase can be expressed as

$$P_{\mathrm{TRX}} = P_{\mathrm{f}} + P_{\mathrm{BB}} + P_{\mathrm{LNA}} + P_{\mathrm{PA}}\,, \tag{7}$$

where P_{f} is the aggregate power consumption of the transceiver blocks (LO, mixer, filters, envelope detector, and baseband amplifier) that are independent of both R_{b} and F_{LNA}. Because the thermal noise and the wideband interference are two independent processes, the minimum required received signal strength [17] can be written considering (6) as follows

$$P_{\mathrm{RSS}} = [k_{\mathrm{B}}T_0L_{\mathrm{SAW}}(B_{\mathrm{SAW}} + (F_{\mathrm{LNA}} - 1)B_{\mathrm{LNA}}) + I_0B_{\mathrm{SAW}}]SINR_{\mathrm{min}}\,, \tag{8}$$

where B_{SAW} is the bandwidth of the SAW filter (see Fig. 2a), and $SINR_{\mathrm{min}}$ (a design constant) is the minimum signal-to-interference-plus-noise ratio that is required to achieve a specific BER value. Because the Q factor of SAW filters can be up to several thousands, B_{SAW} is usually made smaller than B_{LNA} to improve selectivity ($B_{\mathrm{SAW}} = R_{\mathrm{b}}/\eta$). By substituting (8) in (5), we obtain

$$P_{\mathrm{rad}} = L_{\mathrm{B}}SINR_{\mathrm{min}}[k_{\mathrm{B}}T_0L_{\mathrm{SAW}}B_{\mathrm{LNA}}(F_{\mathrm{LNA}} - 1) + \tfrac{1}{\eta}(k_{\mathrm{B}}T_0L_{\mathrm{SAW}} + I_0)R_{\mathrm{b}}]\,. \tag{9}$$

Again by substituting (2)-(4) and (9) in (7) we obtain

$$P_{\mathrm{TRX}} = P_{\mathrm{f}} + \frac{k_{\mathrm{LNA}}}{F_{\mathrm{LNA}}-1} + k_{\mathrm{BB}}R_{\mathrm{b}} + \tfrac{1}{\rho}L_{\mathrm{B}}SINR_{\mathrm{min}}[k_{\mathrm{B}}T_0L_{\mathrm{SAW}}B_{\mathrm{LNA}}(F_{\mathrm{LNA}} - 1) + \tfrac{1}{\eta}(k_{\mathrm{B}}T_0L_{\mathrm{SAW}} + I_0)R_{\mathrm{b}}]\,. \tag{10}$$

Finally, to obtain the formula for the consumed energy per transceived bit, we substitute (10) in (1):

$$E_{\mathrm{bit}} = \frac{P_{\mathrm{f}}}{R_{\mathrm{b}}} + \frac{k_{\mathrm{LNA}}}{(F_{\mathrm{LNA}}-1)R_{\mathrm{b}}} + \frac{P_{\mathrm{f}}T_{\mathrm{UP}}}{N_{\mathrm{b}}} + \frac{k_{\mathrm{LNA}}T_{\mathrm{UP}}}{N_{\mathrm{b}}(F_{\mathrm{LNA}}-1)} + \frac{k_{\mathrm{BB}}T_{\mathrm{UP}}}{N_{\mathrm{b}}}R_{\mathrm{b}} + k_{\mathrm{BB}} + \tfrac{1}{\rho}L_{\mathrm{B}}SINR_{\mathrm{min}}[k_{\mathrm{B}}T_0L_{\mathrm{SAW}}B_{\mathrm{LNA}}(F_{\mathrm{LNA}} - 1)\tfrac{1}{R_{\mathrm{b}}} + \tfrac{1}{\eta}(k_{\mathrm{B}}T_0L_{\mathrm{SAW}} + I_0)]\,. \tag{11}$$

In order to minimize E_{bit}, (11) reveals that the two tradeoffs (between P_{rad} and P_{sens}, and between R_{b} and duty cycle) can actually be reduced to one tradeoff (between F_{LNA} and R_{b}). This tradeoff has an optimum point $(F_{\mathrm{LNA,opt}}, R_{\mathrm{b,opt}})$ at which the total average power consumption is minimum. By finding the zeros of the partial derivatives of (11) with respect to R_{b} and F_{LNA}, we obtain

$$R_{\mathrm{b,opt}}^2 = \frac{N_{\mathrm{b}}}{k_{\mathrm{BB}}T_{\mathrm{UP}}}\left[P_{\mathrm{f}} + \frac{k_{\mathrm{LNA}}}{F_{\mathrm{LNA,opt}-1}} + \tfrac{1}{\rho}k_{\mathrm{c}}\big(F_{\mathrm{LNA,opt}} - 1\big)\right], \tag{12}$$

$$\big(F_{\mathrm{LNA,opt}} - 1\big)^2 = \frac{\rho k_{\mathrm{LNA}}}{k_{\mathrm{c}}}\left(1 + \frac{T_{\mathrm{UP}}}{N_{\mathrm{b}}}R_{\mathrm{b,opt}}\right), \tag{13}$$

where $k_{\mathrm{c}} = L_{\mathrm{B}}SINR_{\mathrm{min}}k_{\mathrm{B}}T_0L_{\mathrm{SAW}}B_{\mathrm{LNA}}$. It is not feasible to analytically solve (12) and (13). Nevertheless, we can still clearly indicate that the value of the optimum $(F_{\mathrm{LNA,opt}}, R_{\mathrm{b,opt}})$ is not affected by whether the system is noise-limited or interference-limited. This is because the optimum is not dependent on I_0 (i.e. how much strong/weak the PSD of the assumed in-channel wideband interference is). In case that the system is interference-limited, it is already known that poor values for F_{LNA} can still be tolerated in order to reduce E_{bit}. However, care should be taken not to surpass $F_{\mathrm{LNA,opt}}$, which is not affected by the value of I_0 and can still be determined from (13). Otherwise, the energy efficiency will start to degrade. To gain more insight from (11)-(13), a numerical example is given in Section III considering the two situations, noise-limited and interference-limited systems.

B. RF Envelope Detector-Based Transceiver

One of the drawbacks of the previous architecture is that it does not support a multi-channel operation. A conventional transceiver architecture [18] that supports the multi-channel operation is shown in Fig. 2(b). The RX section is based on a conventional heterodyne architecture with an image-rejection filter and a free-running LO. The LO is digitally controlled (DCO) and periodically calibrated as in [19], assuming in this analysis that—after calibration—the resulted frequency drift can be neglected. In other words, the resulted IF signal lies in the middle of the IF filter (i.e. $B_{\mathrm{IF}} = R_{\mathrm{b}}/\eta$). However, the analysis needs to take the power budget of the LO into consideration for two reasons. The first one is that LOs always exhibit some level of phase noise, and periodic calibrations of free-running DCOs do not even improve their phase noise performance [18]. The second reason is that the radio spectrum (operating frequency band) is always shared with other interfering nodes as well as with different communicating systems. Combining phase noise impairments with strong adjacent undesired signals leads to the reciprocal mixing phenomenon (see Fig. 4), which results in interference coupled into the desired signal. In many WSN applications, the available frequency band is usually divided into a specific number of operating channels with a minimum channel spacing in between in order to avoid adjacent-channel

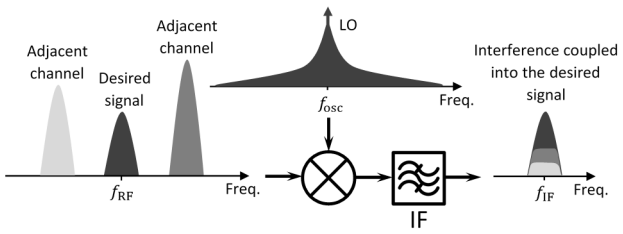

Fig. 4. Reciprocal mixing phenomenon.

interference caused by the aforementioned phenomenon. Therefore, the previous analysis is partially repeated here but with an additional tradeoff to be taken into consideration. This additional tradeoff is between the power dissipation in the LO and the phase noise tolerance which, in the case of ring oscillators [20], is expressed as

$$\mathcal{L}(\Delta f) \approx \frac{7.33 k_{\mathrm{B}} T_0}{P_{\mathrm{osc}}} \left(\frac{f_{\mathrm{osc}}}{\Delta f}\right)^2 , \qquad (14)$$

where $\mathcal{L}$ is the phase noise (expressed in logarithmic scale in dBc/Hz) at an offset frequency Δf from the nominal oscillation frequency f_{osc}. For a given WSN application, f_{osc} and the channel spacing (i.e. Δf) are already specified. Because we are concerned about the phase noise level at an adjacent channel that belongs to the same communicating system, we rewrite (14) as follows:

$$\mathcal{L}_{\mathrm{adj}} = \mathcal{L}(\Delta f_{\mathrm{adj}}) = \frac{k_{\mathrm{PN}}}{P_{\mathrm{osc}}} , \qquad (15)$$

where Δf_{adj} corresponds to the channel spacing, and $k_{\mathrm{PN}} = 7.33 k_{\mathrm{B}} T_0 (f_{\mathrm{osc}}/\Delta f_{\mathrm{adj}})^2$ is a design constant (expressed in watt /Hz).

Similar to (7), the power consumption in the TRX during the transceiving phase is expressed by

$$P_{\mathrm{TRX}} = P_{\mathrm{f}} + P_{\mathrm{BB}} + P_{\mathrm{LNA}} + P_{\mathrm{PA}} + 2P_{\mathrm{osc}} , \qquad (16)$$

where P_{f} now represents the aggregate power consumption of the transceiver blocks (mixers, filters, envelope detector, and baseband amplifier) that are independent of R_{b}, F_{LNA}, and P_{osc}. The factor 2 in front of P_{osc} is because the LO is turned on in the TX as well as in the RX during the transceiving phase. The two existing adjacent channels (as depicted in Fig. 3) are mutually independent as well as independent from the thermal noise and the assumed in-channel wideband interference. For simplicity, we assume that the adjacent-channel interference is modelled as a zero-mean Gaussian process, so that $SINR_{\min}$ can still be obtained from the same BER formula for the case of non-coherent OOK demodulation [21]. Because envelope detection removes the phase and frequency content from the demodulated signal, we assume that the BER performance is not affected for received signals that are corrupted by phase noise. The minimum required received signal strength in (8) can then be rewritten for the case of the heterodyne architecture considering (6) as

$$\begin{aligned} P_{\mathrm{RSS}} &= \left(k_{\mathrm{B}} T_0 F_{\mathrm{LNA}} B_{\mathrm{IF}} + I_0 B_{\mathrm{IF}} + 2\mathcal{L}_{\mathrm{adj}} \frac{P_{\mathrm{rad}}}{L_{\mathrm{loss}}} B_{\mathrm{IF}}\right) SINR_{\min} \\ &= \frac{1}{\eta}\left(k_{\mathrm{B}} T_0 F_{\mathrm{LNA}} + I_0 + 2\mathcal{L}_{\mathrm{adj}} \frac{P_{\mathrm{rad}}}{L_{\mathrm{loss}}}\right) R_{\mathrm{b}} SINR_{\min} , \end{aligned} \qquad (17)$$

where L_{loss} is the minimum allowable link loss between neighboring nodes (taking into consideration the antenna gains of the TX and RX), which depends on how dense the WSN is. The factor 2 in the third term inside the parentheses of (17) is due to the assumption of two existing adjacent channels. Equation (17) considers the worst-case scenario by assuming that the two existing adjacent channels are from two neighboring nodes geographically located in the closest possible position, resulting in L_{loss}. Moreover, these two nodes, which belong to the same communicating system, transmit at a power level equal to P_{rad}. Accordingly, (9)-(11) must be rewritten considering (15)-(17) as follows:

$$P_{\mathrm{rad}} = (k_{\mathrm{B}} T_0 F_{\mathrm{LNA}} + I_0) \left(\frac{\eta}{L_{\mathrm{B}} SINR_{\min} R_{\mathrm{b}}} - \frac{2k_{\mathrm{PN}}}{L_{\mathrm{loss}} P_{\mathrm{osc}}}\right)^{-1} , \qquad (18)$$

$$\begin{aligned} P_{\mathrm{TRX}} = {} & P_{\mathrm{f}} + k_{\mathrm{BB}} R_{\mathrm{b}} + \frac{k_{\mathrm{LNA}}}{F_{\mathrm{LNA}} - 1} + 2P_{\mathrm{osc}} \\ & + \frac{1}{\rho}(k_{\mathrm{B}} T_0 F_{\mathrm{LNA}} + I_0) \left(\frac{\eta}{L_{\mathrm{B}} SINR_{\min} R_{\mathrm{b}}} - \frac{2k_{\mathrm{PN}}}{L_{\mathrm{loss}} P_{\mathrm{osc}}}\right)^{-1} , \end{aligned} \qquad (19)$$

$$\begin{aligned} E_{\mathrm{bit}} = {} & \frac{P_{\mathrm{f}} + 2P_{\mathrm{osc}}}{R_{\mathrm{b}}} + \frac{k_{\mathrm{LNA}}}{(F_{\mathrm{LNA}} - 1) R_{\mathrm{b}}} + \frac{k_{\mathrm{BB}} T_{\mathrm{UP}}}{N_{\mathrm{b}}} R_{\mathrm{b}} \\ & + \frac{k_{\mathrm{LNA}} T_{\mathrm{UP}}}{N_{\mathrm{b}}(F_{\mathrm{LNA}} - 1)} + \frac{(P_{\mathrm{f}} + 2P_{\mathrm{osc}}) T_{\mathrm{UP}}}{N_{\mathrm{b}}} + k_{\mathrm{BB}} \\ & + \frac{1}{\rho}(k_{\mathrm{B}} T_0 F_{\mathrm{LNA}} + I_0) \left(\frac{\eta}{L_{\mathrm{B}} SINR_{\min}} - \frac{2k_{\mathrm{PN}} R_{\mathrm{b}}}{L_{\mathrm{loss}} P_{\mathrm{osc}}}\right)^{-1} . \end{aligned} \qquad (20)$$

From (20), E_{bit} minimization for the heterodyne architecture shows that combing all the three tradeoffs (P_{rad} vs. P_{sens}, duty cycle vs. R_{b}, and $\mathcal{L}$ vs. P_{osc}) yields an optimum point ($F_{\mathrm{LNA,opt}}, R_{\mathrm{b,opt}}, P_{\mathrm{osc,opt}}$) at which the total average power consumption is minimum. As in the previous analysis, finding this optimum analytically is not feasible. Due to space limitations, we have not included the partial derivatives of (20) with respect to F_{LNA}, R_{b}, and P_{osc}. From the partial derivatives, we indicate, as opposed to the previous case, that the PSD level of the in-channel wideband interference does influence the optimum values for the all three design parameters F_{LNA}, R_{b}, and P_{osc}. This outcome is true because the two neighboring interferers, which belong to the same communicating system, transmit at a power level equal to P_{rad} as we assumed earlier in this analysis. For more insight, a numerical example is given in the next section in which the optimum point is determined numerically for a specific WSN application.

III. Numerical Example and Disscussion

The two analyses in the previous section have resulted in a set of equations (11)-(13), and (20), that give a general insight on the optimization process. However, they are not completely intuitive without considering practical scenarios and applications. Therefore, to numerically determine the optimum design and operating parameters (instantaneous data rate, LNA noise figure NF, LO power budget, required radiated power, and RX sensitivity) for both transceiver architectures, values of several corresponding design constants are retrieved from [13] (a frequently-cited publication) and replaced in the equations, keeping in mind all the assumptions and conditions that have been stated throughout the analysis.

A. RF Envelope Detector-Based Transceiver

In the case of an RF envelope detector-based transceiver (RF ED), a numerical example, based on Table I, is first carried out for the situation of noise-limited systems (NLS). Afterwards, it is repeated again for the situation of interference-limited systems (ILS) in which the PSD of the wideband interference is assumed 30 dB greater than the thermal noise (–174 dBm/Hz). Fig. 5 shows the optimization of R_{b} and NF to obtain $E_{\mathrm{bit,min}}$ for the situation of ILS. Due to space limitation, the situation of NLS is not depicted as the coordinates (R_{b} and NF) of the optimum

point are not affected by the value of I_0, as mentioned earlier in Section II-A. Nevertheless, the energy efficiency of both situations is given in Table II.

A 6-MHz band is available at the 916-MHz operating frequency. Assuming $\eta = 1$, R_b is then upper limited by 5 Mbps, leaving 0.5 MHz for guard bands. Moreover, a SAW filter with a Q factor of 1000 [22] can have a 3-dB bandwidth as small as 900 kHz, lower limiting R_b (from the energy efficiency perspective) by 900 kbps. In fact, fixing the SAW filter bandwidth at 900 kHz and decreasing R_b beyond this lower limit do not decrease E_{bit} in any case. The practical limits on R_b result in a practical optimum point instead of the theoretical one as depicted in Fig. 5. Additionally, as opposed to our paper, E_{bit} was reported in [13] based on a different definition which did not consider the impact of the startup time on the energy efficiency in case the duty-cycling technique is employed.

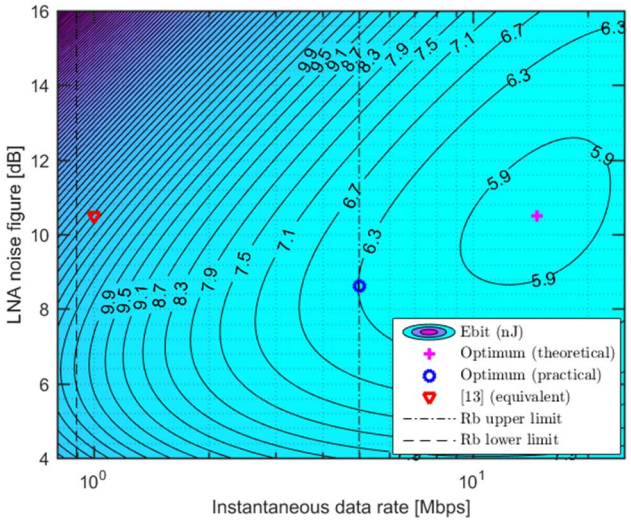

Fig. 5. Consumed energy per transceived bit as a function of instantaneous data rate and LNA noise figure for the RF ED architecture in the ILS situation.

TABLE I. DESIGN CONSTANTS FOR RF ED AND HETERODYNE ARCHITECTURES.

Design Constant	Architecture	Value and Unit	Ref
P_f	RF ED	0.92 mW	[13]
	Heterodyne	0.22 mW	[13, 23]
k_{LNA}	Both	3.6 mW	[13]
N_b	Both	50 bits	[13]
η	Both	1	Assumed
ρ	Both	5%	[13]
B_{LNA}	RF ED	90 MHz	[13]
L_{SAW}	RF ED	3.5 dB	[13]
T_{UP}	Both	60 µsec	[13]
$SINR_{min}$	Both	16 dB	[13]
f_{osc}	RF ED	916 MHz	[13]
	Heterodyne	2.4 GHz	Assumed
L_B	RF ED	60 dB	Assumed
	Heterodyne	55 dB	
k_{BB}	Both	3x10^{-11} watt/bps	[13]
I_0	RF ED	-144 dBm/Hz	Assumed
	Heterodyne	-123 dBm/Hz	
Δf_{adj}	Heterodyne	5 MHz	Assumed
k_{PN}	Heterodyne	6.8x10^{-15} watt/Hz	Assumed
L_{loss}	Heterodyne	50 dB	Assumed

TABLE II. NUMERICAL RESULTS FOR RF ED ARCHITECTURE.

		$R_{b,opt}$ (Mbps)	NF_{opt} (dB)	$P_{rad,opt}$ (dBm)	$P_{sens,opt}$ (dBm)	$E_{bit,min}$ (nJ)
Theoretical	***NLS***	14.7	10.5	-4.8	-64.8	2.6
	ILS			4.3		5.8
Practical	***NLS***	5.0	8.6	-6.9	-66.9	3.1
	ILS			0		6.3
[13] Equivalent	***NLS***	1.0	10.5	-4.8	-64.8	9.4
	ILS			-3.1		12.6

Therefore, we have used the reported power-breakdown results from [13] with our E_{bit} definition to obtain the equivalent point which is plotted in Fig. 5, and reported in Table II as well. Comparing the two practical optimum points with the corresponding equivalent ones for both situations, an approximate energy efficiency improvement of 3 to 5 dB can still be achieved.

From Fig. 5, we can indicate that operating on a higher instantaneous data rate (as long as it is practically feasible) is not only more energy-efficient (up to a point), but also it is safer (from the perspective of the resulted energy efficiency) in case of a deviation in the circuit design. This is because the gradient of E_{bit} with respect to NF is more gradual on higher instantaneous data rates.

For power consumption in the baseband circuits, we have only considered that of the ADC. For a better energy efficiency performance, the power consumption in the digital circuits (e.g. microprocessor) must be taken into consideration because it does affect the optimum point. In fact, the more power-hungry the microprocessor is, the lower the instantaneous data rate and the better the noise figure should be implemented.

B. Conventional Heterodyne-Based Transceiver

In the case of a conventional heterodyne architecture, we repeat the numerical example from Table I for the two situations, NLS and ILS. In both, the operating RF is assumed to belong to the 2.4-GHz ISM band. Therefore, the value of I_0, in the case of ILS, is chosen to represent the PSD of a 100-mW IEEE 802.11g signal attenuated by a typical propagation loss of 70 dB at the receiving node, resulting in I_0 = -53 dBm/Hz - 70 dB = -123 dBm/Hz. In the analysis of the heterodyne architecture, P_{osc} is excluded from P_f, resulting in $P_f = 0.12$ mW [13]. However, the power consumption of two mixers (0.1 mW [23]) need to be included, making $P_f = 0.22$ mW. A minimum distance of 3 meters, which corresponds to a 50-dB free-space path loss, is assumed to separate the sensor nodes.

Due to a channel spacing of 5 MHz, R_b is then upper limited by 5 Mbps. Table III summarizes the optimum design and operating parameters for the two situations. As opposed to the previous architecture, the optimum does vary with the level of the existing wideband interference. However, when the system is ILS, the energy efficiency becomes less sensitive to any deviation on R_b, NF, or P_{osc}. For example, a ±10% deviation on all these three parameters barely increases E_{bit} by 0.8%. This is because E_{bit} in interference-limited systems is dominated by the required radiated power which itself is determined by the requirement of beating strong wideband interference, hence, resulting in a big difference in $E_{bit,min}$ values between NLS and ILS, which is clearly indicated in Table III.

TABLE III. NUMERICAL RESULTS FOR HETERODYNE ARCHITECTURE.

	$R_{b,opt}$ (Mbps)	NF_{opt} (dB)	$P_{osc,opt}$ (mW)	$P_{rad,opt}$ (dBm)	$P_{sens,opt}$ (dBm)	$E_{bit,min}$ (nJ)
NLS	2.37	18.1	0.013	-19.6	-76.2	0.7
ILS	0.64	20.0	0.16	6.1	-79.9	128.5

Similar to the previous case, the power consumption of the digital circuits (e.g. microprocessor) need to be considered along with the ADC as it influences the coordinates of the optimum point. Moreover, the processing load of calibrating the DCO is moved from the RF transceiver to the microprocessor causing more power consumption in the digital circuits section.

IV. CONCLUSION

Two theoretical analyses for determining the minimum total average power consumption in a symmetric system have been presented. The analyses have been carried out on the RF envelope detection and the conventional heterodyne architectures, resulting in two models, in which the optimum parameters for the instantaneous data rate, the receiver noise figure, and the local oscillator power budget have been analytically determined. Numerical examples on both models have been applied considering two situations, noise-limited and interference-limited systems. It has been shown that operating the first architecture on higher instantaneous data rates, as long as it is practically feasible, is safer from the energy efficiency perspective. In the second architecture, the optimum parameters vary with the level of an existing wideband interference, as opposed to the first architecture. However, the energy efficiency becomes less sensitive to the deviation of the parameters in case of interference-limited systems. For further research, the linearity of the receiver (SFDR) and the frequency uncertainty of the LO need to be considered to produce more accurate models. The obtained numerical results are then to be confirmed through experimental prototyping.

ACKNOWLEDGMENT

This work is supported by the Dutch Technology Foundation (STW) through the Slow Wireless project, STW project no. 13769.

REFERENCES

[1] T. Cuzanauskas, A. Medeisis, Y. Haddad, A. Anskaitis, L. Cremene, J. Sydor, O. Holland, and M. Nekovee, "Interference-aware power coordination game for ISM bands," in *Proceedings of the 9th International Conference on Cognitive Radio Oriented Wireless Networks and Communications, CROWNCOM*, Oulu, Finland, June 2014, pp. 389–394.

[2] I. Stojmenovic, *Handbook of sensor networks: Algorithms and architectures*. John Wiley & Sons, 2005.

[3] J. Long, W. Wu, Y. Dong, Y. Zhao, M. Sanduleanu, J. Gerrits, and G. Van Veenendaal, "Energy-efficient wireless front-end concepts for ultra lower power radio," in *Proceedings of the Custom Integrated Circuits Conference*, San Jose, CA, USA, Sep. 2008, pp. 587–590.

[4] S. Ehsan and B. Hamdaoui, "A survey on energy-efficient routing techniques with QoS assurances for wireless multimedia sensor networks," *IEEE Communications Surveys and Tutorials*, vol. 14, no. 2, pp. 265–278, May 2012.

[5] T. Rault, A. Bouabdallah, and Y. Challal, "Energy efficiency in wireless sensor networks: A top-down survey," *Computer Networks*, vol. 67, pp. 104–122, July 2014.

[6] J. Rabaey, J. Ammer, T. Karalar, S. Li, B. Otis, M. Sheets, and T. Tuan, "PicoRadios for wireless sensor networks: The next challenge in ultra-low power design," in *Digest of Technical Papers - IEEE International Solid-State Circuits Conference*, San Francisco, CA, USA, Feb. 2002, pp. 200–201+195.

[7] M. Srivastava, "Power-aware communication systems," in *Power Aware Design Methodologies*. Springer, 2002, pp. 297–334.

[8] B. Cook, A. Molnar, and K. Pister, "Low power RF design for sensor networks," in *Digest of Papers - IEEE Radio Frequency Integrated Circuits Symposium*, Long Beach, CA, USA, June 2005, pp. 357–360.

[9] R. Dutta, R. Zee, M. Bentum, and A. Kokkeler, "Choosing optimum noise figure and data rate in wireless sensor network radio transceivers," in *IEEE International Conference on Communications*, Kyoto, Japan, June 2011.

[10] Y. Li, D. Qiao, Z. Xu, D. Xu, F. Miao, and Y. Zhang, "Energy-model-based optimal communication systems design for wireless sensor networks," *International Journal of Distributed Sensor Networks*, vol. 2012, 2012.

[11] M. Lont, D. Milosevic, and A. van Roermund, *Wake-up receiver based ultra-low-power WBAN*. Springer, 2014.

[12] M. Pedram and Q. Wu, "Design considerations for battery-powered electronics," in *Proceedings - Design Automation Conference*, New Orleans, LA, USA, June 1999, pp. 861–866.

[13] D. Daly and A. Chandrakasan, "An energy-efficient OOK transceiver for wireless sensor networks," *IEEE Journal of Solid-State Circuits*, vol. 42, no. 5, pp. 1003–1010, May 2007.

[14] N. Kim, T. Austin, D. Blaauw, T. Mudge, K. Flautner, J. Hu, M. Jane Irwin, M. Kandemir, and V. Narayanan, "Leakage current: Moore's law meets static power," *Computer*, vol. 36, no. 12, Dec. 2003.

[15] T. C. Randall, "A low-power, reconfigurable, pipelined ADC with automatic adaptation for implantable bioimpedance applications," Ph.D. dissertation, EECS, Univ. of Tennessee, Knoxville, TN, Dec. 2014.

[16] T. Tran, C. Boon, M. Do, and K. Yeo, "Ultra low power low noise amplifier designs for 2.4 GHz ISM band applications," Ph.D. dissertation, Dept. of Elect. & Electron. Eng, Nanyang Tech. Univ., Singapore, July 2012.

[17] A. F. Molisch, *Wireless communications*, 2nd ed. Wiley Publishing, 2011.

[18] P. P. Mercier and A. P. Chandrakasan, *Ultra-low-power short-range radios*. Springer, 2015.

[19] N. Pletcher, S. Gambini, and J. Rabaey, "A 52 μW wake-up receiver with -72 dBm sensitivity using an uncertain-IF architecture," *IEEE Journal of Solid-State Circuits*, vol. 44, no. 1, pp. 269–280, Jan. 2009.

[20] R. Navid, T. Lee, and R. Dutton, "Minimum achievable phase noise of RC oscillators," *IEEE Journal of Solid-State Circuits*, vol. 40, no. 3, pp. 630–636, March 2005.

[21] B. Sklar, *Digital communications fundamentals and applications*, 2nd ed. Prentice Hall NJ, 2001.

[22] T. Kimura, M. Kadota, and Y. Ida, "High Q SAW resonator using upper-electrodes on grooved-electrodes in LiTaO3," *in IEEE MTT-S International Microwave Symposium Digest*, Anaheim, CA, USA, May 2010, pp. 1740–1743.

[23] Q. Zhang, X. Kuang, and N. Wu, "An ultra-low-power RF transceiver for WBANs in medical applications," *Journal of Semiconductors*, vol. 32, no. 6, June 2011.